



**HAL**  
open science

## Comparison of different numerical methodologies to derive fragility curves of RC buildings with soil-structure interactions

Thomas Ulrich, Caterina Negulescu, Evelyne Foerster, Hormoz Modaressi, Samuel Auclair

### ► To cite this version:

Thomas Ulrich, Caterina Negulescu, Evelyne Foerster, Hormoz Modaressi, Samuel Auclair. Comparison of different numerical methodologies to derive fragility curves of RC buildings with soil-structure interactions. EUROODYN 2011, Eighth International Conference on Structural Dynamics, Jul 2011, Leuven, Belgium. hal-00591773

**HAL Id: hal-00591773**

**<https://brgm.hal.science/hal-00591773>**

Submitted on 10 May 2011

**HAL** is a multi-disciplinary open access archive for the deposit and dissemination of scientific research documents, whether they are published or not. The documents may come from teaching and research institutions in France or abroad, or from public or private research centers.

L'archive ouverte pluridisciplinaire **HAL**, est destinée au dépôt et à la diffusion de documents scientifiques de niveau recherche, publiés ou non, émanant des établissements d'enseignement et de recherche français ou étrangers, des laboratoires publics ou privés.

# Comparison of different numerical methodologies to derive fragility curves of RC buildings with soil-structure interactions

T. Ulrich<sup>1</sup>, C. Negulescu<sup>1</sup>, E. Foerster<sup>1</sup>, H. Modaressi<sup>1</sup>, S. Auclair<sup>1</sup>

<sup>1</sup>BRGM (French Geological Survey), Natural Risks and CO2 Storage Safety Division, 3 Avenue Claude Guillemin, 45060 Orléans Cedex 2, France

email: t.ulrich@brgm.fr, c.negulescu@brgm.fr, e.foerster@brgm.fr, h.modaressi@brgm.fr, s.auclair@brgm.fr

**ABSTRACT:** In order to assess the physical vulnerability of buildings, the general methodology consists in deriving fragility curves, representing the probabilities of exceeding some predefined structural damage states as a function of a parameter representing the hazard levels (e.g. PGA). In general, these curves do not account for soil-structure interactions (SSI). This paper intends to quantify their influence on the dynamic response of inelastic building-foundation systems and on the resulting fragility curves. We will compare the results obtained with two different numerical methodologies, considering a combination of two different RC building typologies (low-rise/high-rise) and underlying layered soils (shear wave velocities ranging from 100 to 300 m/s):

1) A two-step analysis, in which the bed-rock response is first propagated in superficial layers using CyberQuake program. The resulting waveform is transferred at the building foundation through an empirical adjustment factor. Then, the nonlinear dynamic response of a 3D building model is computed with the finite element program SeismoStruct, with link elements to account for soil deformation patterns (rocking and sway).

2) A one-step analysis, in which the soil and building are modeled at once using the finite element software GEFDYN, considering 1D simplified building models (MDOF stick) over a 2D soil model.

The fragility curves computed in this paper, compared with the ones derived from fixed base models, will permit to quantify the effects (favorable or not) of SSI with respect to various relevant parameters identified.

**KEY WORDS:** SSI; fragility curves; inter-story drift.

## 1 INTRODUCTION

The interaction between the structure and the soil during the dynamic loading is named soil-structure interaction (SSI). Two mechanisms of interaction take place between the structure, foundation and soil: 1) inertial interaction, developed in the structure due to its own vibrations gives rise to base shear and moment, which in turn cause displacements of the foundation relative to free-field and 2) kinematic interaction, explained by the presence of stiff foundation elements on or in soil that cause foundation motions to deviate from free-field motion as a result of ground motion incoherence, wave inclination, or foundation embedment (Stewart et al., 1999). Inertial effects can be described by frequency dependent foundation impedance functions expressed by a complex number: its real part is related to the rigidity and its imaginary part to the damping capacity. The effective damping is a summation of two sources: radiation damping (transmitted by the structure to the soil) and hysteretic damping of the soil. The impedance can be represented by a Kelvin Voigt Model composed of a viscous

dashpot and a spring connected in parallel. There are different techniques and software to evaluate the SSI response. Generally, for these studies the soil and the structure are computed in the same model. Anyway, some studies show that when the slab may be assumed rigid, the soil spring techniques appear sufficient compared to more sophisticated techniques such as the SASSI code (Nien et al., 2001). In this study both techniques are tested to calculate the SSI response.

## 2 MODEL DESCRIPTION AND ANALYSIS

Two different approaches to the SSI phenomenon have been considered. Figure 1 presents a simplified representation of each model: 1) the two-step approach - soil analysis using CyberQuake program (Foerster & Modaressi, 2007) and structure analysis using SeismoStruct program (SeismoSoft, 2003) and 2) the one-step approach - soil and building in the same model using GEFDYN software. The different colours of the accelerograms indicate its changes.

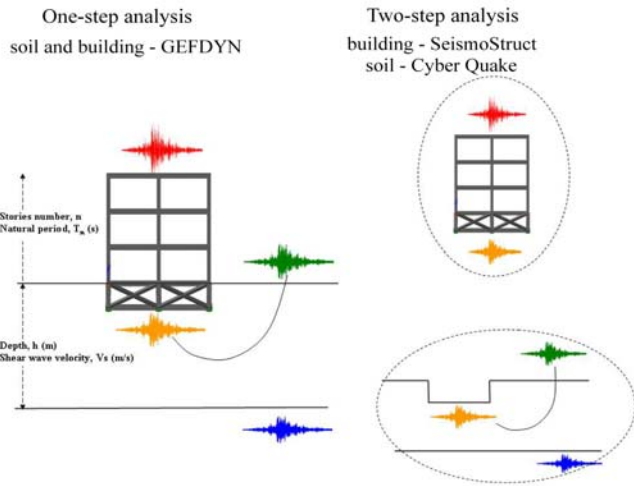


Figure 1. One-step and two-step SSI analysis

### 2.1 Two-step analysis

The global problem of SSI is split into two different phases. In Phase 1, the wave amplification in surface layers is estimated by convolution of engineering bedrock time-histories through different soil profiles. The shear wave velocities of the soil profiles are  $V_s = 100, 200$  and  $300$  m/s and the depths,  $h$ , are 5 and 10 m. 6 one-layer soil profiles over rigid bedrock are considered.

During Phase 2, we estimate the building behavior under the seismic loading. The target buildings are analyzed twice: first considering rigid base conditions (encasing link) and second considering a movement between the structure and the soil (springs and dashpots link). In this study, two RC buildings with natural periods of vibrations equal to 0.1s and 0.5s were analyzed. A very rigid basement system having 2m depth is considered for each structure.

The motion resulting from the Phase 1 is the free-field motion. This motion is different from the motion under the foundation. The input motion for the Phase 2 is the motion under the foundation system. This motion is obtained by applying an empirical adjustment factor to the free-field motion. This adjustment factor results from investigations of the observed records at free-field and at foundation level during the 1995 Hygoken Nanbu Earthquake (Yasui, 1997; AIJ, 2004) and from the results of analysis performed to investigate the characteristics of input motions on frequency (IAEA, 2003; AIJ, 2004).

### 2.2 One-step analysis

SSI is also investigated in a unified approach, with the finite element software Gefdyn. In such analyses, the wave propagation from bedrock through the soil layers to the top of the structure is modeled in one step.

Contrary to the two-step analysis, soil layers are modeled within a 2D mesh (quadrangle elements) and the structure is

represented by simple spring-mass models, whose characteristics have been adjusted to fit with the linear behavior of the Seismostruct structures. Figure 2 presents the geometry used in the analyses:

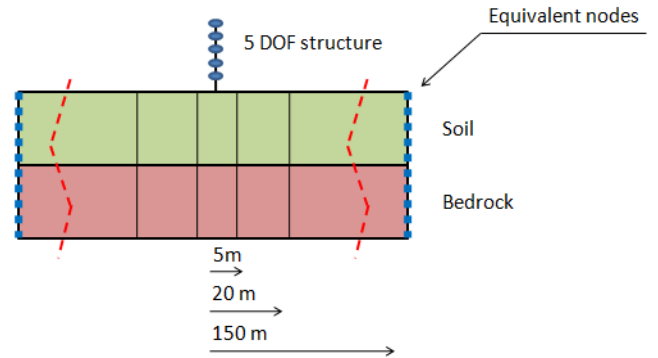


Figure 2. Geometry of the model.

We assume that the incident wave propagates vertically, so that the mesh is very much refined in that direction to avoid numerical dispersion (25 nodes per wave length  $\lambda$  for a maximum frequency of 20 Hz). Moreover, the soil right beneath the structure, up to 5m away from it, is finely meshed to catch the soil-structure effects more accurately (25 nodes per  $\lambda$ ). Then, up to 20m away, the soil is less finely meshed (10 nodes per  $\lambda$ ), and finally the soil stretches up to 150m away from the building with a very coarse mesh, to avoid spurious boundary condition effects. This decreasing pattern in the mesh permits to save computational time. Equivalent boundaries conditions are imposed on the vertical boundaries to prevent the incident wave to distort near the boundaries.

As no non-linear effects are considered in these analyses, the impulsional response of the model is computed and is then convoluted with the bedrock accelerograms to compute the inter-storey drift (ISD).

### 2.3 Building description

Regarding the two-step approach, two 3D RC buildings with 1 and 5 stories respectively, are defined for dynamic time-history analyses. The height floor is 3m. The basement is considered a technical one having 2m height. The foundation is continuous on the building contour and is rigidified by truss elements. The rigidity of the truss elements is calibrated in order to have the same natural period of vibration as for the structure without basement. For each model, the very regular structure consists of 2 spans and 2 bays of 4m each. Cross sections of the columns are rectangular (55 x 55 cm for the 0.1s model and 40 x 30 cm for the 0.5s one). The beams have constant sections: 50 x 35 cm for 0.1s model and 50 x 20 cm for 0.5s model. Buildings' properties are presented in Table 1. The 0.1s model is designed in order to be about 100 times stiffer than the 0.5s model. The frames are made of cast in place reinforced concrete having concrete strength  $f_c = 30$ MPa, Young's modulus for the concrete was taken equal to 27,500MPa. The reinforcement yielding stress is  $f_y = 500$ MPa. Both structures are modelled with Seismostruct software. The beams and columns are inelastic frame elements capable to take into consideration geometrical and material

nonlinearities. The sectional stress-strain state of beam-column elements is obtained through the integration of the nonlinear uniaxial material response of the individual fibres in which the section has been subdivided, fully accounting for the spread of inelasticity along the member length and across the section depth. The structures have been constructed to have the natural period of vibration 0.1 times the stories number, namely 0.1 and 0.5 seconds.

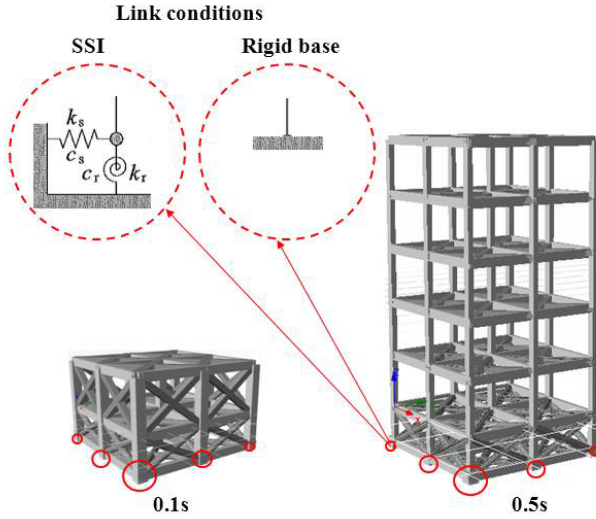


Figure 3. Models for non-linear time history analysis (two-step approach)

For rigid base analysis all the base nodes have encasing link while for the SSI analysis the flexible link (permitting rotation and translation) are used, as presented in Figure 3. The properties of the link elements (rigidity and damping) are calculated using empirical relationship presented in the next paragraph.

Table 1. Properties of the building models

Natural period of vibration T(s)	Mass M(t)	Rigidity K(t/m)	Beam section (cm)	Column section (cm)
0.1	1405	5555000	55x55	50x35
0.5	246	49330	40x30	50x20

#### 2.4 Impedance matrix

The impedance matrix can be conceptually viewed as an assemblage of springs and dashpots (Pecker, 2007). The expressions for stiffness and damping of equivalent springs for rigid foundation on a stratum over rigid bedrock (IAEA, 2003) are presented for various degrees of freedom:

$$K_S = \frac{8GR}{2-\nu} \left( 1 + \frac{1}{2} \frac{R}{h} \right), \quad h/R > 1, \quad \text{horizontal direction of motion} \quad (1)$$

$$K_R = \frac{8GR^3}{3(1-\nu)} \left( 1 + \frac{1}{6} \frac{R}{h} \right), \quad 4 > h/R > 1, \quad \text{rocking direction of motion} \quad (2)$$

$$K_V = \frac{4GR}{1-\nu} \left( 1 + 1.28 \frac{R}{h} \right), \quad h/R > 2, \quad \text{vertical direction of motion} \quad (3)$$

where  $h$  is the substratum thickness;  $R$ , an equivalent radius for a rectangular foundation;  $G$  and  $\nu$ , respectively the shear modulus and Poisson's ratio of the soil.

$$C_S = C_1 K_H R \sqrt{\rho/G}, \quad \text{horizontal equivalent damping coefficient} \quad (4)$$

$$C_R = C_2 K_R R \sqrt{\rho/G}, \quad \text{rocking equivalent damping coefficient} \quad (5)$$

$$C_V = C_3 K_V R \sqrt{\rho/G}, \quad \text{vertical equivalent damping coefficient} \quad (6)$$

where  $C_1=0.5$ ;  $C_2=0.3/(1-B_\phi)$ ;  $B_\phi=3(1-\nu)I_0/8\rho R^5$ ;  $\rho$  is the soil bulk density and  $I_0$ , the mass moment of inertia.

For each foundation motion, the reduced radiation damping factor of a soil is calculated from the damping coefficient determined using the above relationships:

$$\xi_{SSI} = 0.5 \frac{C}{2K} \quad (7)$$

where  $C$  and  $K$  are the damping and stiffness coefficients respectively. The 0.5 factor is intended to take into account the fact that the actual radiation damping is less than that for a 'regular' half-space, due to wave's reflection in horizontal soil layers. The overall soil damping factor is obtained as:

$$\xi_S = \xi_g + \xi_{SSI} \quad (8)$$

where  $\xi_g$  is the hysteretic soil damping. This value is limited to 30%.

#### 2.5 Adjustment factor

The dynamic soil-structure interaction effect can be considered by the means of the adjustment factor  $H_{SSI}(\omega)$  (AIJ, 2004), which is defined as follows:

$$\begin{aligned} |H_{SSI}(\omega)|^2 &= \frac{|U_{fh}|^2}{|U_{GL}|^2} = \frac{1}{1+2\eta\delta_d^2}, \quad \delta_d < 1 \quad \text{and} \\ |H_{SSI}(\omega)|^2 &= \frac{|U_{fh}|^2}{|U_{GL}|^2} = \frac{1}{1+2\eta}, \quad \delta_d \geq 1 \end{aligned} \quad (9)$$

where  $\eta=d/l$ ;  $\delta_d = \omega/\omega_d$ ;  $\omega_d = (\pi V_s)/(2d)$ , and  $l$  is the foundation width;  $d$ , the foundation embedment depth;  $U_{fh}$ , the foundation motion;  $U_{GL}$ , the free field motion;  $V_s$ , the shear wave velocity of the soil adjacent to the side wall. The

foundation geometry of the studied models is the following: plane dimensions:  $8\text{m} \times 8\text{m}$ ,  $l=8\text{m}$  and  $d=2\text{m}$  ( $\eta=1/4$ ).

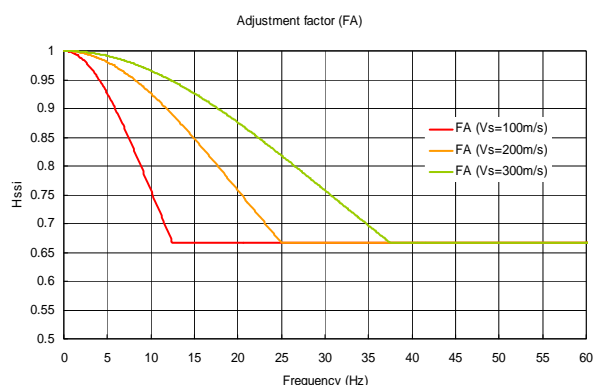


Figure 4. Adjustment factor (FA) of the embedded foundation for three soil conditions:  $V_s=100, 200$  and  $300\text{m/s}$

Figure 4 presents the adjustment factor for the embedded foundation and for three layers having shear wave velocities of 100, 200 and 300 m/s respectively. The adjustment factor is multiplied by the free-field motion in order to obtain motion under the foundation. The motion under the foundation is then used as input motion in the SSI dynamic time histories analyses of the structure performed with Seismostruct.

### 2.6 Input motions for dynamic analyses

A total number of 246 strong-motions were used for performing dynamic analyses. The histogram of the PGA values is presented in Figure 5. As the structural modeling was faster for the one-step approach, a larger number of calculations were performed in this case. In total, we used 246 strong-motion records as input to time-history analyses for the one-step approach and 108 only for the two-step one.

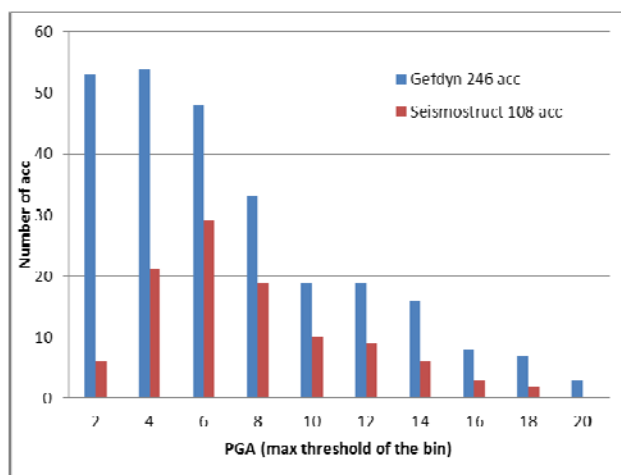


Figure 5. Histogram of the PGA ( $\text{m/s}^2$ ) values for the time-histories used for dynamic analyses

### 2.7 Fragility curves derivation

The fragility curves are used to represent the probability that a given damage level is reached (or exceeded) for any

given level of ground motion characterized by PGA (intensity) value. For each simulation performed (one or two-step and rigid base or SSI), the highest inter-storey drift ratio (ISDR) was extracted as the structure response to the seismic input. An advantage of using the ISDR to evaluate the damage level of a building is that this variable is fairly intuitive and was widely used in previous studies.

The fragility curves are based on the analytical work of Shinozuka et al., 2000 [11], who expresses the fragility curve in the form of a two-parameter lognormal distribution function. The two parameters of the distribution represent the median and the lognormal standard deviation and are computed so as to maximize the likelihood function (Gehl et al., 2009 [3]).

## 3 RESULTS AND DISCUSSIONS

The various steps considered in this study to assess SSI effects are: 1) computation with rigid base hypothesis, 2) computation considering SSI for different combinations of soil profile and structure, and 3) evaluation of SSI effects. Generally, the following parameters were analyzed: a) fundamental frequency of the structure, b) PGA at base and top of the structure, c) Spectral Acceleration  $SA(T)$  at base and top of the structure, d) Structure's transfer function with regard to input's frequency content, e) Displacement at base and top of the structure, f) Bending moments and forces in structure's elements, etc. The obtained results are commented first considering the frequency changes of the models and second, considering the fragility curves developed for rigid base and SSI cases and by both one-step and two-step approaches. For frequency domain analyses, the result that seems to be more explicit and that is presented in the following figures is the transfer function between the top and the base of the structure. The figures of the earthquake records are processed using Viewwave software coded by T. Kashima (2005, Building Research Institute, Tsukuba, Japan).

Figure 6 presents the results obtained for the 0.1s model considering one of the strong-motion records and the two-step approach. For each substratum thickness  $h$ , we plot the Rigid base response in red and the SSI ones in blue ( $V_s$  equal to 100 m/s), pink ( $V_s=200$  m/s) and orange ( $V_s=300$  m/s). On this figure, we note that due to SSI effects, the natural period changes from 0.1s (Rigid base condition) to 0.22s for  $V_s=100$  m/s.

This change in natural period almost vanishes with the increasing shear wave velocity: 0.2s for 100m/s, 0.14s for 200m/s and 0.12s for 300m/s. This trend is more visible on the 5m-thick soil profile than on the 10m-thick one. Here, the SSI effect is well explained by the properties of the structures (very big mass and rigidity) and of the soil profile (low share wave velocity).

Figure 7 shows the period modification of the structure considering SSI effect for the 0.5s model and two-step approach. In this case the changes in the natural periods are less visible for the soil profile with different shear wave velocities and even for the different thicknesses.

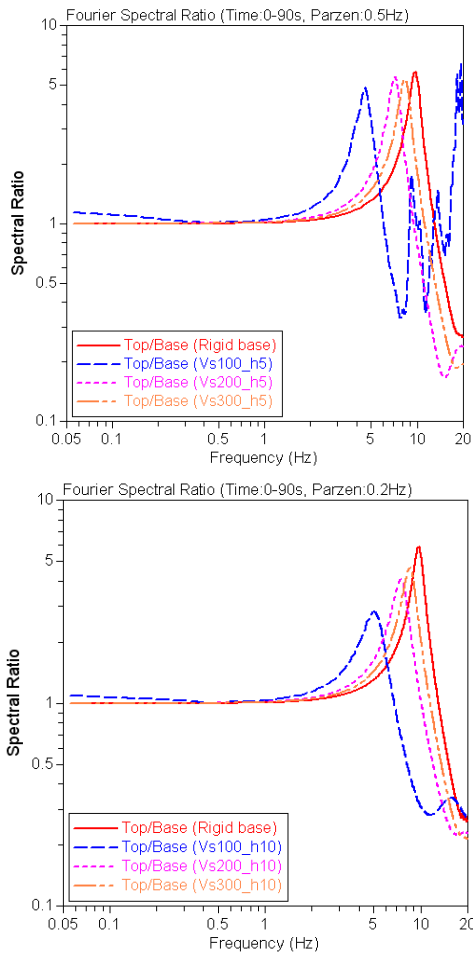


Figure 6. Spectral Ratios computed between top and base of the 0.1s model for three soil conditions ( $V_s=100, 200$  and  $300$  m/s) and two soil thicknesses ( $h=5$  m and  $10$  m)

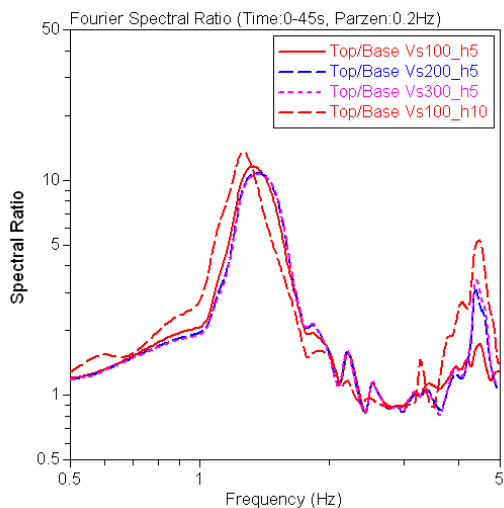


Figure 7. Spectral Ratios computed between top and base of the 0.5s model for three soil conditions ( $V_s=100, 200$  and  $300$  m/s) and two soil thicknesses ( $h=5$  m and  $10$  m)

Contrary to the spectral analyses carried out for the two-step approach, the impulsional response of the drift of the structure have been directly analysed for the second model (Gefdyn):

the results of these investigations (Figure 8) confirm globally the conclusion drawn for the first model (Seismostruct).

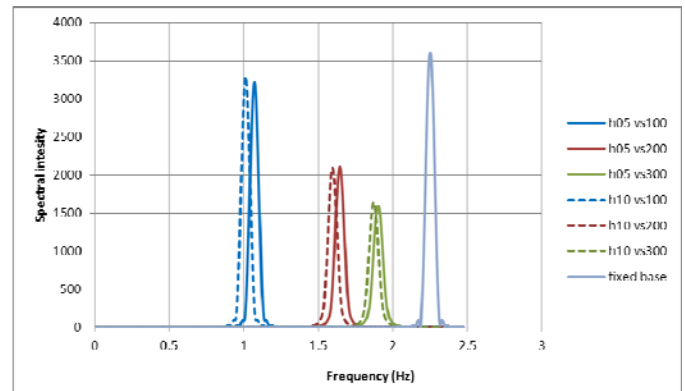


Figure 8. Influence of SSI on the drift of the 5 story building (spectral intensity, computed from the one-step approach).

In fact, the fundamental frequency of the system {soil, structure} is lower when the soil is softer. The results of the simulations with a 10m-thick soil are quite similar with those of 5m-thick soil, but the effect of the SSI seems a little bit stronger in the 1<sup>st</sup> case, contrary to the observations made on the first model. Globally, SSI effects seem to be more predominant in the one-step approach, if we look at the changes in the fundamental frequency observed easily even for the 5 story building. Finally, the observed difference between heights of the intensity peaks is mainly due to the damping produced by SSI, which is greater when  $V_s$  increases.

For the 0.1s model, the fragility curves developed when considering SSI effects show damage amplification for both type of approaches (one-step and two-step). This phenomenon is explained by the rocking movement that the SSI phenomenon induces to the structure. In this case, the inter-storey drift parameter is not adequate for measuring the damage of the building unless the component displacement corresponding to the rocking is extracted from the total displacement obtained at the top of the building. The displacement corresponding to the rocking movement is related to the increase in the rigid movement that does not influence the damage of the structure, but increases the total top displacement of the structure hence the inter-storey drift.

For the 0.5s model, the rocking component of the motion is less important and the inter-storey drift has been used for calculating the fragility curves for both one-step and two-step approaches.

Figures 9 and 10 show the fragility curves obtained for the 0.5s model with two-step and one-step approaches respectively. For the two-step approach, we note that the SSI effect reduces the probability of damage occurrence for PGA values superior to  $8 \text{ m/s}^2$ . In the one-step case, the SSI effect reduces the probability of damage occurrence. In Figure 11, we compare the curves obtained by one-step and two-step approaches.

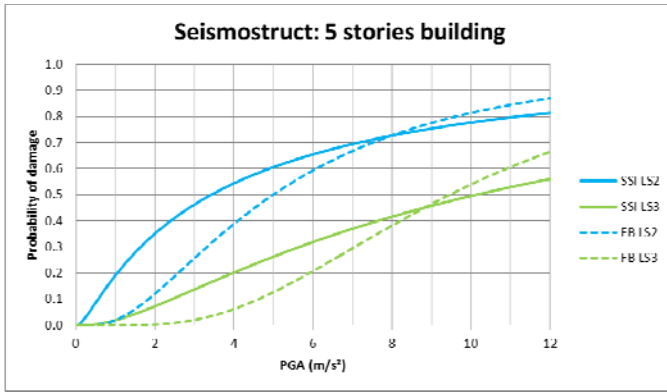


Figure 9. Fragility curves for 5 story buildings developed using two-step approach

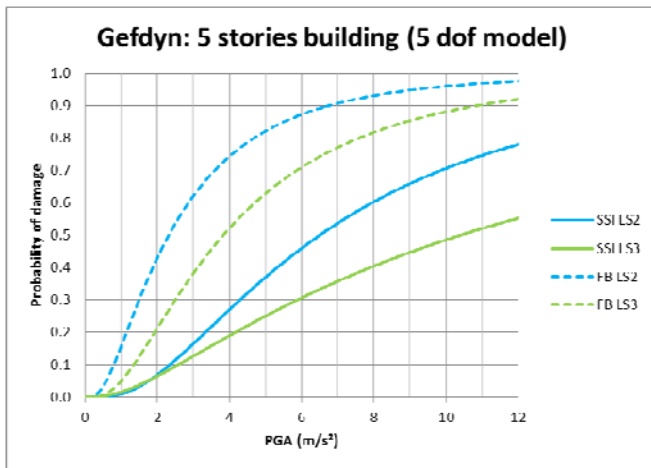


Figure 10. Fragility curves for 5 story buildings developed using one-step approach

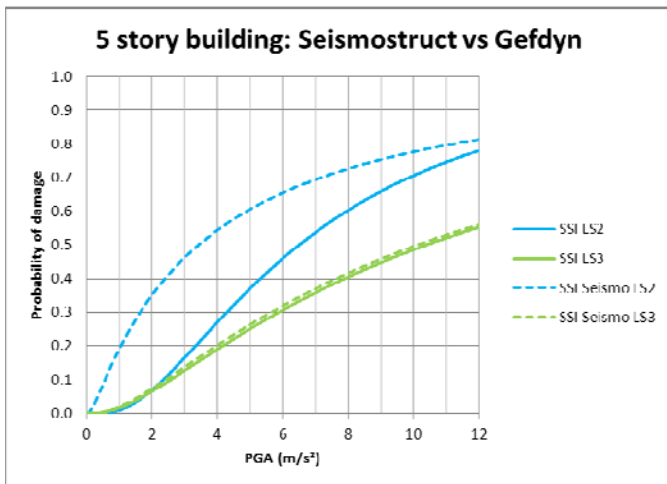


Figure 11. Comparison between the fragility curves developed using one-step and two-step approaches

#### 4 CONCLUSIONS

The results obtained from dynamic time histories in terms of transfer functions show a good match with the SSI period calculated using empirical relation. For the 0.1s model, the change in the rigid base period due to the SSI effect is

obvious. It's difficult to draw general conclusions about the influence of the soil foundation thickness on the fundamental period of the structure from the 2 configurations analysed in this study (5m and 10m). However, previous researches [7] have shown that the SSI effect diminishes with the increasing soil thickness  $h$ . The amplitude of the Fourier spectral ratio decreases with increasing  $h$ . If considering only frequency content, there is no concrete evidence of SSI effects for the 0.5s models when performing a two-step analysis.

Regarding fragility curves for the 0.1s model for both one-step and two-step approaches, the SSI effect increases the probability of observing damage. However, this result is not realistic and can be explained by the fact that ISD parameter is not adequate for measuring the damage of the building. Indeed, part of the displacement at the top of the building is produced by a rigid body movement that does not affect the damage of the structure. We must also note that linear assumption for soil behavior under such a building is not realistic: the role of confinement pressure due to the building heavy weight for soils right underneath cannot be neglected. Consequently, the soft soil under such a structure may exhibit nonlinear behaviour. As a consequence, plastic yielding and damping effects may result from the rocking of the structure, which will decrease the importance of this movement.

For the 0.5s structure and the Gefdyn model (one-step approach), the SSI effects decrease the probability of damage occurrence. For the Seismostruct model, the SSI effects diminish the probability of damage occurrence for PGA superior to  $8\text{m/s}^2$  and increase it otherwise.

Generally the resulting damages are less important for two-step analyses because of the nonlinear behavior considered for the structure that tends to reduce the drift (due to material damping). For the one-step approach, the structure behavior is assumed to be linear.

#### ACKNOWLEDGMENTS

This work was supported by the brgm research department under grant RISR17-VULNERISC.

#### REFERENCES

- [1] Aubry D., Chouvet D., Modaressi A., Modaressi H., GEFDYN : Logiciel d'Analyse de Comportement Mécanique des Sols par Eléments Finis avec Prise en Compte du Couplage Sol-Eau-Air, Manuel scientifique, Ecole Centrale Paris, LMSS-Mat (1986).
- [2] AIJ Architectural Institute of Japan. (2004). AIJ Recommendations for Loads on Buildings, Recommendations and Commentaries, Chapter 7 Seismic loads, 54 pages.
- [3] Gehl P., Seyedi D., Douglas J., Khair M. (2009). Introduction of Fragility Surfaces for a More Accurate Modeling of the Seismic Vulnerability of Reinforced Concrete Structures, COMPDYN 2009 - ECCOMAS Thematic Conference on Computational Methods in Structural Dynamics and Earthquake Engineering M. Papadrakakis, N.D. Lagaros, M. Fragiadakis (eds.) Rhodes, Greece.
- [4] IAEA-TECDOC-1347. (2003), Consideration of external events in the design of nuclear facilities other than nuclear power plants, with emphasis on earthquakes, IAEA, ISBN 92-0-102803-2.
- [5] Kashima, T. (2005). IISEE, Building Research Institute, Tsukuba, Japan <http://iisee.kenken.go.jp/staff/kashima/viewwave.html>.
- [6] Foerster, E. & Modaressi, H. (2007). Nonlinear numerical method for earthquake site response analysis II- case studies. Bulletin of Earthquake

- Engineering, 5 (3): 325-345, 2007..
- [7] Negulescu C., Roullé A., Foerster E., Ulrich T., Yoshimi M. (2010). Effect of Soil Structure Interaction on the dynamic response of the building, 14ECEE, Ohrid, paper 1248, 8 pages.
  - [8] Nien, C. T., Aejaz, A. and Calvin, Y. W. (2001). Soil-Structure Interaction Effects on Seismic Response of ISFSI Slabs. *Transactions, SMIRT 16*, paper 1256, 8 pages.
  - [9] Pecker, A. (2007). Soil Structure Interaction. *Advanced Earthquake Engineering Analysis*, Chapter 3, Edt A. Pecker, CISM N°494, Springer, 33-42.
  - [10] SeismoSoft: SeismoStruct (2003). A computer program for static and dynamic nonlinear analysis of framed structures, <http://www.seismosoft.com>.
  - [11] M. Shinozuka, Q. Feng, J. Lee, T. Naganuma, Statistical analysis of fragility curves. *Journal of Engineering Mechanics*, ASCE, 126(12), 1224–1231, 2000.
  - [12] Stewart, J. P., Fenves, G. L. and Seed, R. B. (1999). Seismic soil-structure interaction in buildings. I: Analytical methods, *J. Geotech Engrg.*, ASCE, 125(1), 26-37.
  - [13] Yasui, Y. (1997). Relationship between Building Damage and Strong Motion Records - Soil-Building Interaction . *AIJ*, pp.67–86.